AIRS: ARIEL IR Spectrometer status

Jérôme Martignac, Jérôme Amiaux, Michel Berthé,

Christophe Cara, Cyrille Delisles, et al.

Published version information:

Citation: J Martignac et al. AIRS: ARIEL IR spectrometer status. Proc SPIE 12180 (2022): 1218012. Is in proceedings of: SPACE TELESCOPES AND INSTRUMENTATION 2022: OPTICAL, INFRARED, AND MILLIMETER WAVE, Montreal, CANADA, 17-22 Jul 2022.

DOI: 10.1117/12.2628920

AIRS: ARIEL IR spectrometer status

Jérôme Martignac, Jérôme Amiaux, Michel Berthé, Christophe Cara, Cyrille Delisles, et al.

Jérôme Martignac, Jérôme Amiaux, Michel Berthé, Christophe Cara, Cyrille Delisles, Achrène Direk, Luc Dumaye, Jean Fontignie, Alain Goestschy, Benoît Horeau, Norma Hurtado, Duc-Dat Huyn, Grégory Kaszubiak, Pierre-Olivier Lagage, Isabelle Le Mer, Michel Lortholary, Vincent Moreau, Salima Mouzali, Patrick Mulet, François Nico, Thibault Pichon, Lena Provost, Diana Renaud, Victor Schwartz, Michel Talvard, Thierry Tourrette, François Visticot, Axel Arhancet, Damien Bachet, Nicolas Berton, Mickael Lacroix, Hervé Le Provost, Olivier Tellier, Anne Philippon, Clémence De Jabrun, Jean-Pierre Dubois, François Langlet, Dylan Le Claire, Benoît Lecomte, Marc Ollivier, Stéphane Tosti, Vincent Lapeyrère, Marion Bonafous, Jérôme Parisot, Jean-Michel Reess, Didier Zegadanin, Jean-Philipe Beaulieu, Virginie Batista, Pierre Drossart, Salma Fahmy, Delphine Jollet, Ludovic Puig, Thierry Tirolien, Pascale Danto, Gilles Hervet, Oceane Maisonnave, Paul Eccleston, Georgia Bishop, Rachel Drumond, Andrew Caldwell, Martin Caldwell, Lucile Desjonqueres, Martin Whalley, Enzo Pascale, Gianluca Morgante, Mauro Focardi, Emanuele Pace, Anna Maria Di Giorgio, "AIRS: ARIEL IR spectrometer status," Proc. SPIE 12180, Space Telescopes and Instrumentation 2022: Optical, Infrared, and Millimeter Wave, 1218012 (27 August 2022); doi: 10.1117/12.2628920

Event: SPIE Astronomical Telescopes + Instrumentation, 2022, Montréal, Québec, Canada

AIRS: ARIEL IR Spectrometer status

Jérôme Martignac*[a], Jérôme Amiaux[a], Michel Berthé[a], Christophe Cara[a], Cyrille Delisle[a], Achrène Direk[a], Luc Dumaye[a], Jean Fontignie[a], Alain Goetschy[a], Audrey Goujon[a], Benoît Horeau[a], Norma Hurtado[a], Duc-Dat Huyn[a], Grégory Kaszubiak[a], Pierre-Olivier Lagage[a], Isabelle Le Mer[a], Michel Lortholary[a], Vincent Moreau[a], Salima Mouzali[a], Patrick Mulet[a], François Nico[a], Thibault Pichon[a], Lena Provost[a], Diana Renaud[a], Victor Schwartz[a], Michel Talvard[a], Thierry Tourrette[a], François Visticot[a], Axel Arhancet[b], Damien Bachet[b], Nicolas Berton[b], Mickael Lacroix[b], Hervé Le Provost[b], Olivier Tellier[b], Anne Philippon[c], Clémence Dejabrun[c], Jean-Pierre Dubois[c], François Langlet[c], Dylan Le-Claire[c], Benoît Lecomte[c], Gilles Morinaud[c], Marc Ollivier[c], Stéphane Tosti[c],Vincent Lapeyrere[d], Marion Bonafous[d],Jérôme Parisot[d], Jean-Michel Reess[d], Didier Zeganadin[d],Jean-Philippe Beaulieu[e], Virgine Baptista[e], Pierre Drossart[e], Salma Fahmy[f], Delphine Jollet[f], Ludovic Puig[f], Thierry Tirolien[f], Pascale Danto[g], Gilles Hervet[g], Oceane Maisonnave[g], Paul Eccleston[h], Rachel Drummond[h], Georgia Bishop[h], Andrew Caldwell[h], Martin Caldwell[h], Lucile Desjonqueres[h], Martin Whalley[h], Enzo Pascale[i], Gianluca Morgante[j], Mauro Focardi[l], Emanuele Pace[k], Anna Maria Di Giorgio[l],
and the ARIEL consortium.

[a] : Université Paris-Saclay, Université Paris Cité, CEA, CNRS, AIM, 91191, Gif-sur-Yvette, France;
[b] : Université Paris-Saclay, CEA, IRFU, F-91191 Gif-sur-Yvette, France;
[c] : Institut d'Astrophysique Spatiale, université Paris Saclay, CNRS, Orsay, France ;
[d] : LESIA, Observatoire de Paris, Université PSL, CNRS, Sorbonne Université, Université de Paris, Meudon, France;
[e] : Institut Astrophysique de Paris, Paris, France ;
[f] : ESA – ESTEC, Noordwijk, Netherlands ;
[g] : CNES, Toulouse, France ;
[h] : RAL Space, Science & Technology Facilities Council (STFC), Rutherford Appleton Laboratory, Harwell Campus, Didcot, Oxon, UK;
[i] : Universita degli Studi di Roma "La Sapienza" , Roma, Italy ;
[j] : INAF OAS, Bologna, Italy; [k] : INAF OAA, Firenze, Italy; [l]: INAF IAPS, Roma, Italy.

Abstract

AIRS is the infrared spectroscopic instrument of ARIEL: Atmospheric Remote-sensing Infrared Exoplanet Large-survey mission selected in March 2018 as the Cosmic Vision M4 ESA mission and planned to be launched in 2029 by an Ariane 6 from Kourou toward a large amplitude orbit around L2 for a 4 year mission.
Within the scientific payload, AIRS will perform transit spectroscopy of over a 1000 of exoplanets to complete a statistical survey, including gas giants, Neptunes, super-Earths and Earth-size planets around a wide range of host stars. All these collected spectroscopic data will be a major asset to answer the key scientific questions addressed by this mission: what are the exoplanets made of? How do planets and planetary system form? How do planets and their atmospheres evolve over time?
The AIRS instrument is based on two independent channels covering the CH0 [1.95-3.90] µm and the CH1 [3.90-7.80] µm wavelength range with prism-based dispersive elements producing spectrum of low resolutions R>100 in CH0 and R>30 in CH1 on two independent detectors. The spectrometer is designed to provide spectrum Nyquist-sampled in both spatial and spectral directions to limit the sensitivity of measurements to the jitter noise and intra pixels pattern during the long (10 hours) transit spectroscopy exposures. A full instrument overview will be presented covering the thermal mechanical design of the instrument functioning in a 60 K cold environment, up to the detection and acquisition chain of both channels based on 2 HgCdTe detectors actively cooled down below 42 K. This overview will present updated information of phase B2 studies in particular with the early manufacturing of prototype for key elements like the optics, focal-plane assembly and read-out electronics as well as the results of testing of the IR detectors up to 8.0 µm cut-off.

Keywords: Exoplanet, Spectroscopy, Transit, Atmospheres, IR Detectors, Payload

* Corresponding Author; jerome.martignac@cea.fr

Space Telescopes and Instrumentation 2022: Optical, Infrared, and Millimeter Wave, edited by
Laura E. Coyle, Shuji Matsuura, Marshall D. Perrin, Proc. of SPIE Vol. 12180,
1218012 · © 2022 SPIE · 0277-786X · doi: 10.1117/12.2628920

1. INTRODUCTION

The Ariel Infra-Red Spectrometer (AIRS) is the science instrument of the Ariel Payload providing Low Resolution Spectrum of the observed targets over broad IR wavebands covering the [1,95-7,8] µm range.
After a description of the ARIEL mission and a presentation of the AIRS consortium, this paper provides an overview of the full instrument design covering in details all sub-systems, and to finish the latest advances in terms of manufacturing and testing.

2. THE ARIEL MISSION

2.1 The ARIEL Science

Thousands of exoplanets have now been discovered with a huge range of masses, sizes and orbits: from rocky Earth-size planets to large gas giants grazing the surface of their host star (Figure 1, left). However, the essential nature of these exoplanets remains largely mysterious: there is no known, discernible pattern linking the presence, size, or orbital parameters of a planet to the nature of its parent star. We have little idea whether the chemistry of a planet is linked to its formation environment, or whether the type of host star drives the physics and chemistry of the planet's birth, and evolution (Figure 1, right). Progress with these science questions demands a large, unbiased spectroscopic survey of exoplanets. The ARIEL mission has been conceived and designed to conduct such a survey and to explore the nature of exoplanet atmospheres and interiors and, through this, the key factors affecting the formation and evolution of planetary systems in our galaxy.

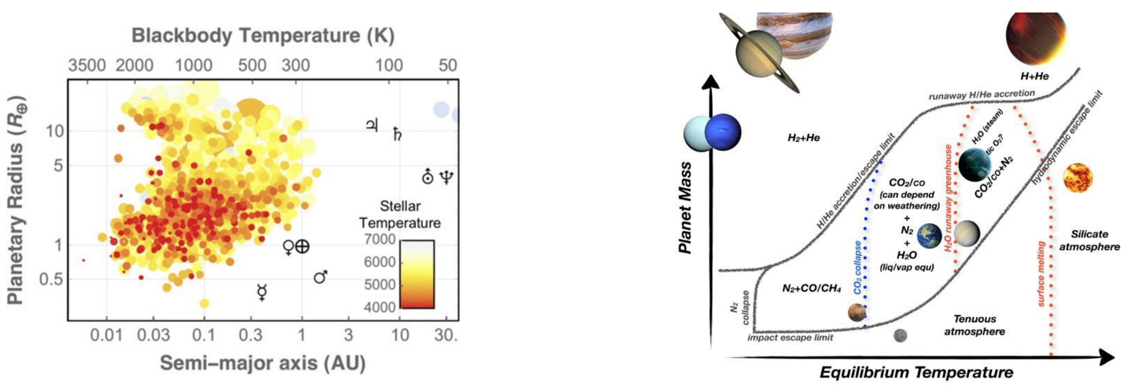

Figure 1. Left: Currently known exoplanets, plotted as a function of distance to the star (up to 30 AU) and planetary radii. The graph suggests a continuous distribution of planetary sizes – from sub-Earths to super-Jupiters – and planetary temperatures that span two orders of magnitude. Right: Schematic summary of the various classes of atmospheres [01]. Only the expected dominant species are indicated, other (trace) gases will be present. Each line represents a transition from one regime to another, but these "transitions" need tight calibrations from observations. The axes do not have numerical values as they are unknown. Solar System planets are indicated, together with a lava planet, an Ocean planet and a hot Jupiter. ARIEL will observe planets ranging from the Earth to the super-Jupiter masses, especially warm and hot ones: many atmospheric regime transitions are expected to occur in this domain.

ARIEL will address the fundamental questions:

- *What are exoplanets made of?*
- *How do planets form and evolve?*

through the direct measurement of the atmospheric chemical composition and thermal structure. ARIEL will focus on warm and hot planets, for which the atmospheric composition is more representative of the bulk one.
ARIEL will observe a large number, i.e. ~ 1000, of warm and hot transiting gas giants, Neptunes and super-Earths around a range of host star types using transit spectroscopy in the 1.1-7.8 µm spectral range and multiple-band photometry in the optical. We target in particular warm and hot planets to take advantage of their well-mixed

atmospheres which should show minimal condensation and sequestration of high-Z materials and thus reveal their bulk and elemental composition (especially C, O, N, S, Si). Observations of these exoplanets will allow the understanding of the early stages of planetary and atmospheric formation during the nebular phase and the following few millions years. ARIEL will thus provide a truly representative picture of the chemical nature of the exoplanets and relate this directly to the type and chemical environment of the host star (Figure 1, right).

ARIEL will address the fundamental questions:

- *What are exoplanets made of?*
- *How do planets form and evolve?*

For this ambitious scientific programme, ARIEL is designed as a dedicated survey mission for transit, eclipse and phase-curves spectroscopy, capable of observing a large and well-defined planet sample within its 4-year mission lifetime. Transit and eclipse spectroscopy methods, whereby the signal from the star and planet are differentiated using knowledge of the planetary ephemerides, allow us to measure atmospheric signals from the planet at levels of ~10-100 ppm relative to the star (post-processing) and, given the bright nature of targets, also allows more sophisticated techniques, such as phase curve analysis and eclipse mapping, to give a deeper insight into the nature of the atmosphere (Figure 2). Transit spectroscopy means that no angular resolution is required and detailed performance studies during Phase A and Phase B have demonstrated that a 1-metre class telescope is sufficient to achieve the necessary observations on all the ARIEL targets within the mission lifetime. The satellite is best placed into an L2 orbit to maximise the thermal stability and the field of regard.

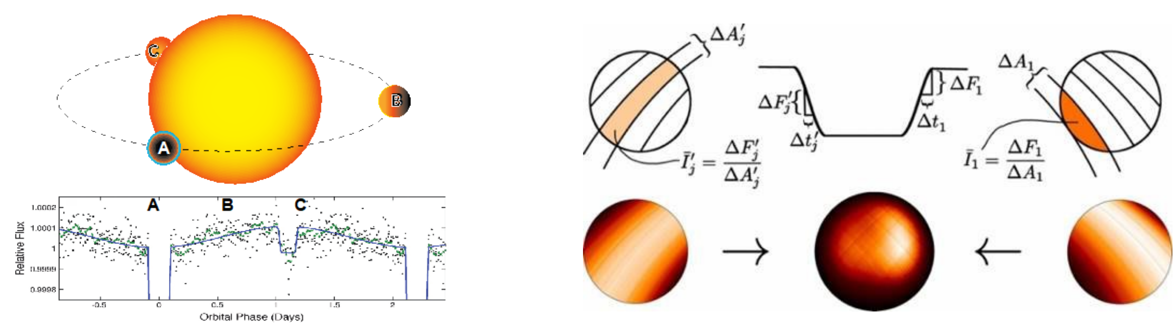

Figure 2. Methods adopted by ARIEL to probe the exoplanet composition and atmospheric structure. Left: phase-curve of the transiting exoplanet HAT-P-7b as observed by Kepler [02]. The transit and eclipse are visible. Right: slice mapping with ingress and egress maps, as well as a combined map of HD189733b at 8 μm. These were achieved with Spitzer [03]

To maximise the science return of ARIEL and take full advantage of its unique characteristics, a four-tiered approach has been considered, where three different samples are observed at optimised spectral resolutions, wavelength intervals and signal-to-noise ratios, and a fourth Tier is considered for bespoke observations of special targets and phase-curves.

2.2 The ARIEL Spacecraft

The ARIEL spacecraft is designed in a modular way, with a service module (SVM) and a payload module (PLM) that can be procured and tested in parallel. ESA is responsible for the overall ARIEL mission. Under an ESA contract, Airbus Defence and Space (ADS) will lead the European industrial consortium building the satellite bus. The ADS Toulouse facility in France will be the main site for designing, manufacturing and integrating the spacecraft elements, while Airbus Stevenage in the UK will lead the engineering of the avionics, radio frequency communication and electrical design of the platform. The ARIEL mission consortium (AMC) funded by national agencies will provide the full ARIEL payload (telescope and instruments). An illustration of the ARIEL spacecraft with a focus on the payload is shown in Figure 3.

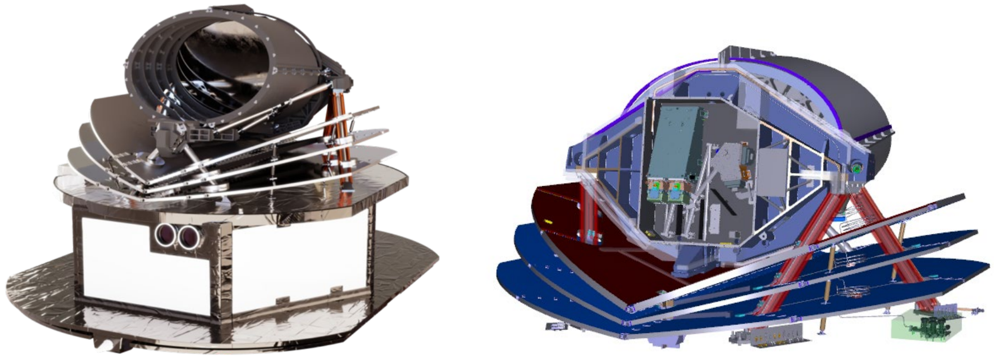

Figure 3. Left: Overview of ARIEL spacecraft with the PLM on top (black part) and the SVM on bottom – Right: PLM overview from the back. The passive radiator of the instrument's cavity is hidden to show the two instruments of the ARIEL mission: the FGS and AIRS.

The main characteristics of the ARIEL Spacecraft depicted in Figure 3 are as follows:

- Elliptical primary mirror: 1.1 x 0.7 meters;
- Mission lifetime: at least 4 years in orbit;
- Payload mass / launch mass: ~500 kg / ~ 1500kg;
- Instrumentation: 3 photometric channels and 3 spectrometers covering continuously from 0.5 to 7.8 microns in wavelength;
- Launch date: 2029;
- Destination: Sun – Earth Lagrange Point 2 (L2);
- Launch vehicle: Ariane 6-2. Launch shared with Comet Interceptor.

The SVM contains all the units required to operate the spacecraft and maintain the payload in its nominal operating conditions. The spacecraft has a wet mass of ~1.2 t and a power generation capability of ~1 kW. 180 Gbit of science data will be generated every week, and are down-linked in 3 ground contacts totaling 14 hrs/week using an X-band system and the 35 m ESTRACK ground stations. The fine pointing requirements achieved by the AOCS system are (3 sigma): APE ≤ 1"; RPE ≤ 200 mas up to 90 s; PDE ≤ 100 mas up to 10 hrs for integrations of 90 s. This is achieved with a Fine Guidance Sensor (FGS, part of the payload instrument suite) and reaction wheels only as the sole actuators (accommodated on dampers, and operated within a narrow angular speed range to minimise any micro-vibrations and avoid exciting structural modes of the S/C).

The PLM design is optimised to fulfil the science requirements while keeping the technical risks and costs within the M4 programmatic constraints of the payload consortium. The baseline integrated payload consists of an all-Aluminium off-axis Cassegrain telescope (primary mirror 1100 mm x 730 mm ellipse) with a re-focussing mechanism accommodated behind the M2 mirror and allows correction for any misalignment generated during the telescope assembly or launch and cool down. The telescope feeds a collimated beam into two separate instrument modules. A combined Fine Guidance System / VIS-Photometer / NIR-Spectrometer contains 3 channels of photometry between 0.50 μm and 1.2 μm, of which two will also be used as a redundant system for providing guidance and closed-loop feedback to the high stability pointing of the spacecraft. The FGS provides simultaneous information on the photometric stability of the target stars. One further low resolution (R = ~10) spectrometer in the 1.2 μm – 1.95 μm waveband, optimized for cloud characterisation, is also accommodated here. The other instrument module, the ARIEL IR Spectrometer (AIRS), provides spectral resolutions of between 30 – 100 for a waveband between 1.95 μm and 7.8 μm. The payload module is passively cooled to ~55 K by isolation from the spacecraft bus via a series of V-Groove radiators; the detectors for the AIRS are the only items that require active cooling to < 42 K via an active Neon JT cooler.

The Ariel mission payload is developed by a consortium of more than 50 institutes from 16 ESA countries – which include the UK, France, Italy, Poland, Belgium, Spain, the Netherlands, Austria, Denmark, Ireland, Norway, Sweden, Czech Republic, Hungary, Portugal, Estonia – plus a NASA contribution. A NASA and JAXA contributions have been confirmed.

This Payload is composed of 2 major items, as illustrated in Figure 4:

- The cold PayLoad Module composed of :
  - Telescope is an optical off-axis Cassegrain telescope system, incorporating the primary mirror M1, secondary mirror at prime focus M2 with a re-focusing mechanism on the M2 mirror (M2M), the M3 and M4 beams to collimate the beam and direct it towards the optical bench and common optics, the telescope structure and the baffles;
  - The Telescope Optical Bench (TOB) / Metering Structure onto which both the telescope items (M1, M2, M3, & M4 mirrors/support structure, Common Optics equipment, Calibration Unit, Cooler Cold head and Passive Thermal Equipment) and the instruments (AIRS and FGS) are mounted;
  - The optical bench, metering structure and telescope mirrors and mechanisms are together referred to as the Telescope Assembly (TA); [04]
  - A set of common optics to split the incoming beam between the AIRS and FGS instruments including the M5 mirror to direct the incoming beam, the dichroic to split the FGS and spectrometer light, formatting optics to inject the light into the spectrometer correctly, and a common calibration source for the payload at the M5;
  - The ARIEL IR Spectrometer (AIRS) to use the light focused by the telescope to perform the primary science objectives of the mission, including all optics and structure plus detectors, cold front-end electronics (CFEE), and interface to the AIRS DCU are extensively described in this paper;
  - The Fine Guidance Sensor (FGS)/Visible Photometer/Near-IR Spectrometer (FGS/VISPhot/NIRSpec), including all optics and dichroics to split into the 4 separate channels, prime and redundant detectors and front-end electronics (FEE);
  - Thermal hardware: active cooler system based on Neon JT cooler, passive radiator for cooling of FGS detectors and associated FEE, V-grooves and support structure to isolate the cold PLM from the warmer SVM and solar thermal loads. [06]
- The Warm Units mounted in the Spacecraft Service Module (SVM):
  - Instrument Control Unit (ICU) [07] [08], which includes a power supply unit (PSU), providing the secondary power lines to A-DCU, and the Command and Data Processing Unit (CDPU) which implements the communication and interface to the TCU and the spectrometer data acquisition and onboard preprocessing;
  - AIR Detector Control Unit (A-DCU) which includes a power and data interface to the ICU, housekeeping & central logic, biasing, data acquisition & pre-processing for the spectrometer and thermal control and monitoring for AIRS;
  - Telescope Control Unit (TCU) managing the Payload Thermal Control stabilization System (TCS), including primary (M1) and secondary (M2) mirrors TCS, the M2 mechanism (M2M) and the P/L On-Board Calibration Source (OBCS);
  - FGS Control Unit (FCU) electronics incorporating the FGS/VISPhot/NIRSpec wFEE, the control and processing electronics and software for determining the pointing from the FGS data and transmitting this information to the spacecraft;
  - Active Cooler System (ACS) composed of the Cooler Control Electronics, the Cooler compressors and the Cooler gas handling panel. [09]

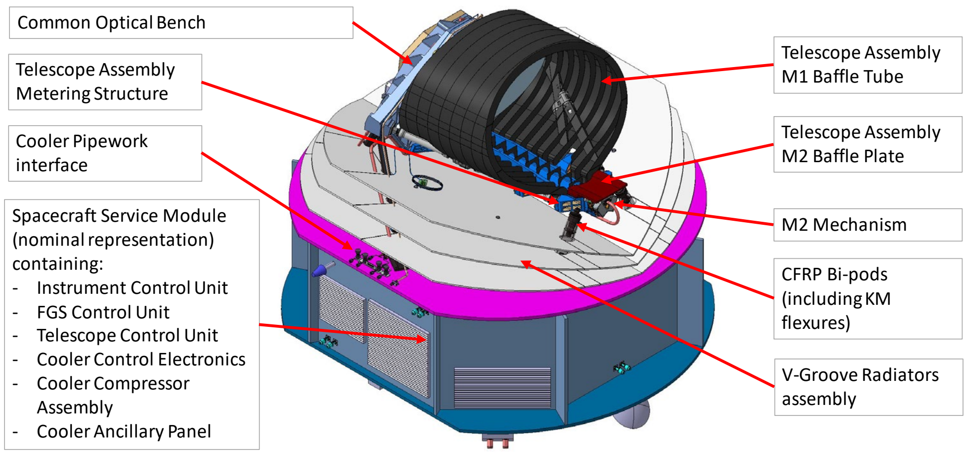

Figure 4. ARIEL payload elements

3. AIRS CONSORTIUM

The AIRS instrument is developed in France by a consortium of scientific laboratories in collaboration with the French Space Agency (CNES) who will be the Lead Funding Agency for this part of the mission and provide experts support. In this consortium, responsibilities are shared as follows:

- 3 laboratories (Département d'Astrophysique, Département d'Ingénierie des Systèmes and Département d'Électronique des Détecteurs et d'Informatique pour la Physique) part of Irfu (Institut de recherche sur les lois fondamentales de l'Univers) of CEA are in charge of the overall project management, system engineering, electrical architecture, product assurance and the design, testing and procurement of the complete detection chain (Focal Plane Assemblies and Detector Control Units, including its firmware);
- Institut d'Astrophysique Spatiale (IAS) part of CNRS is in charge of the overall mechanical, optical and thermal architecture and the design, testing and procurement instruments Optical Bench, including all its optical elements;
- Laboratoire d'Etudes Spatiales et d'Instrumentation en Astrophysique (LESIA) part of CNRS and Observatoire de Paris is in charge of the instrument's calibrations including the development of the relevant test chamber and optical setup.

The instruments detectors are procured for the AIRS instrument from Teledyne Imaging Systems by the European Space Agency.
The cryoharness connecting the warm and cold parts of the instrument will be developed in Canada under the responsibility of the Canadian Space Agency (CSA).

4. AIRS SYSTEM OVERVIEW AND MAIN SPECIFICATIONS

AIRS is the ARIEL scientific instrument providing low-resolution spectroscopy in 2-IR channels (called Channel 0 (CH0) for the [1.95-3.90] µm band and Channel 1 (CH1) for the [3.90-7.80] µm band). It is located at the intermediate focal plane of the telescope + common optical system.

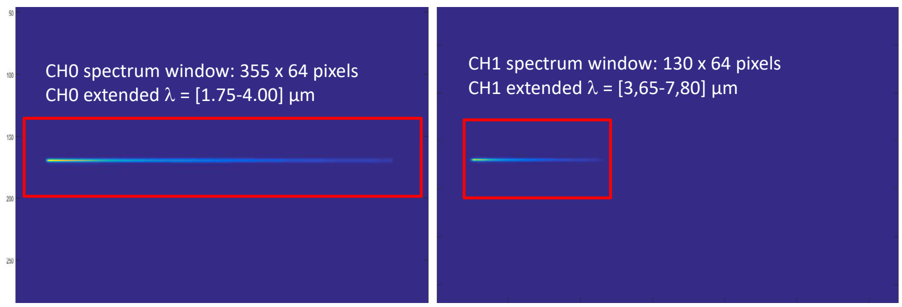

Figure 5. AIRS CH0 spectrum window 355 x 64 pixels and CH1 spectrum window 130 x 64 pixels

The instrument is based on two independent channels (CH0 / CH1) optical paths with prisms dispersive elements producing spectrum of low resolutions R≥100 in CH0 and R≥30 in CH1 on two independent detectors.

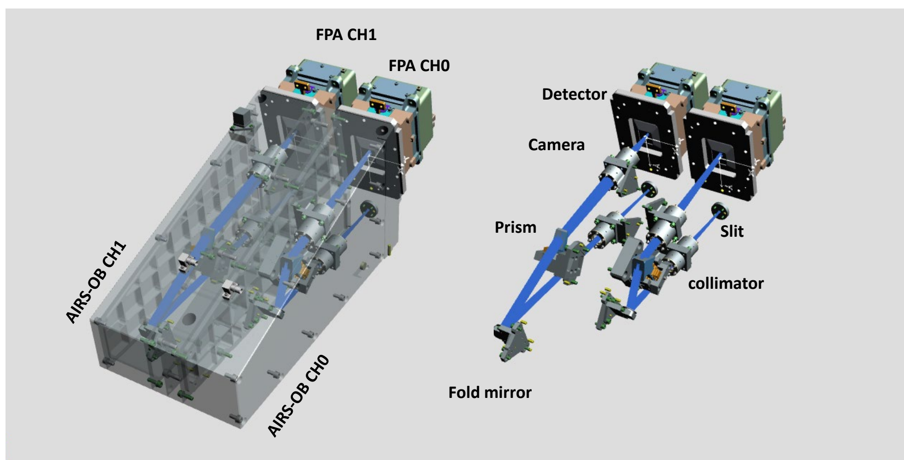

Figure 6. Illustration of the ARIEL Infra-Red Spectrometer

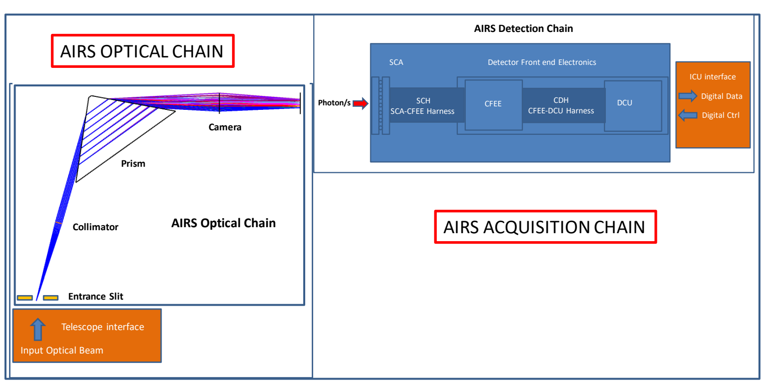

Figure 7. Architectural block diagram of the ARIEL Infra-Red Spectrometer

Ariel Infra-Red Spectrometer (AIRS) is the composed of 2 main functional chains:

- The Optical Chain Function, which is converting the entrance optical object into a spectrum in the image focal plane of the system;

- The Acquisition Chain Function which converts the incoming optical spectrum into digital science data packets that will be sent to the ground through the Instrument Control Unit (ICU) and the SerVice Module (SVM).

AIRS Optical Chain performs slit spectroscopy in two channels (CH0 [1,95-3,90] µm and CH1 [3,90-7,80] µm). The nominal wavebands are extended to [1.75-4.0] µm for CH0 and [3.65-7.80] for CH1 in order to allow band to band and FGS to AIRS cross calibrations. The incoming telescope beams in both channels are limited with a slit (to prevent extra background contamination of the spectra). Both telescope beams are collimated onto a prism dispersive element. The out coming dispersed beams are re-image by camera on the respective CH0 and CH1 detector. In-field stray light control is implemented through polishing residual figure error and contamination control of optical elements.
The AIRS Optical Chain main internal interfaces are with the AIRS-Focal Plane Assembly (optically for spectrum flux and size definition, thermally for passive cool down). The AIRS Optical Chain main external interfaces are with the Payload Module Telescope Optical Bench (TOB) for optical, mechanical and thermal interface.

AIRS acquisition chain performs photon detection of the spectra provided by the AIRS Optical Bench and process them into digital science packets downloaded to the S/C via interface to the ICU.
The AIRS acquisition chain main internal interfaces are with the AIRS-Optical Bench (optically for spectrum flux and size definition, thermally for passive cool down), between Detector and Cold Front-End Electronics (CFEE), and between the CFEE and the AIRS Detector Control Unit (A-DCU) (for Science data transmission, House Keeping and detector sequencer programming control and for processing of the digital codes). The two H1RG detectors (operated in window mode) are not controlled by commonly used SIDECAR electronics but rely on control electronics developed in-house at CEA. The AIRS Detection Chain main external interfaces are with the PLM Cryocooler for the cold finger of the Detector, with the PLM for the Cold to Warm Harness routing and with ICU for clean secondary voltage, TC I/F to S/C and Data packet to S/C Mass Memory.

4.1 AIRS block Architecture

AIRS instrument is composed of four main architectural blocks:

- AIRS Optical Bench (AIRS-OB with 2 optical channels CH0 and CH1);
- AIRS Focal Plane Assembly for Channel 0 and 1 (AIRS-FPA-CH0 and AIRS-FPA-CH1);
- AIRS Cold Front-End Electronics for Channel 0 and 1 (AIRS-CFEE-CH0 and AIRS-CFEE-CH1);
- AIRS Detector Control Unit (A-DCU);
- AIRS Inter Unit Harness (AIRS-IUH).

AIRS-OB and AIRS-FPA and AIRS-CFEE are located on the cold section of the PLM, while the A-DCU is located in the warm part of the SVM.

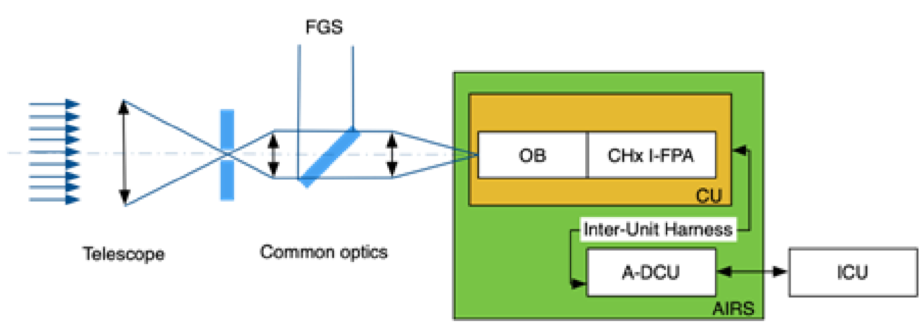

Figure 8. AIRS Block Architecture

5. AIRS OPTICAL DESIGN BASE LINE

AIRS spectrometer interface with the pre-optics (Telescope + COB) in the image focal plane of the pre-optics (see Figure 9). This plane is the object focal plane of AIRS. The focused beam at the AIRS input slits have focal ratios of f/12 (spatial direction) and f/18 (spectral direction).

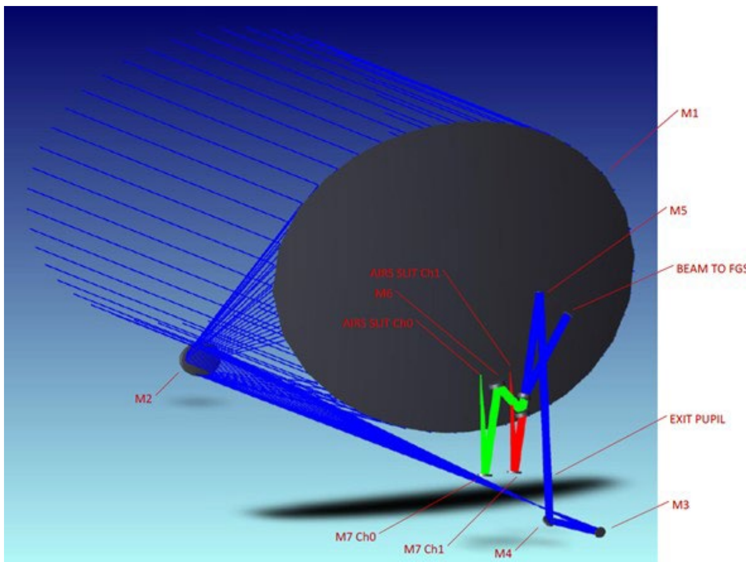

Figure 9. Telescope and Common Optic interface to CH0 & CH1 AIRS Slits

The optical design implements, as baseline, a prism system with 2 independent optical paths CH0 and CH1 with the following configuration:

- An input image of the target in the entrance focal plane of the spectrometer including a large slit which function is to limit the background flux on the detector and act as a field stop;
- A collimator that collimates the incoming beam on the prism;
- A prism which is the dispersive element;
- A camera which function is to re-image the beam on the detector.

The definition of the useful wavelength for each channel is defined as follow:

- Nominal wavebands with full performance:
  - CH0: 1.95-3.9 um
  - CH1: 3.9-7.8 um
- Extension of wavebands for cross calibration between AIRS and FGS/NIRSpec with relaxed performances:
  - CH0: 1.85 - 4.00 µm
  - CH1: 3.65 - 7.80 µm

The detailed Zemax model introduces bi material doublets systems for the Camera and the Collimator (CaF_2/Sapphire) for Ch0 and (CaF_2/ZnSe) for CH1 in order to control the chromatic aberrations. The design is analyzed at the operational temperature of 55 K and the indexes of refraction are defined at this temperature.

With this correction the system is diffraction limited over the nominal useful wavelength range. The diameter of the lenses has been increased above the useful area in order to increase the mechanical resistivity and simplify the mechanical mount design. Moreover, this allows providing an unvignetted beam over the full extended waveband.

The incident angle and apex angle for the prisms parameters are set from the nominal design to meet the performance of spatial and spectral sampling. From those values, the nominal incident angles on both dioptres of the CH0 and CH1 prisms are defined.
The nominal design point is set to sample with 2 pixels the diffraction limited first Airy ring of the system and to provide a linear dispersion of 2 pixels in the focal plane for a $\Delta\lambda$ corresponding to a resolution of 100 at λmin in CH0 and 30 at λmin in CH1.

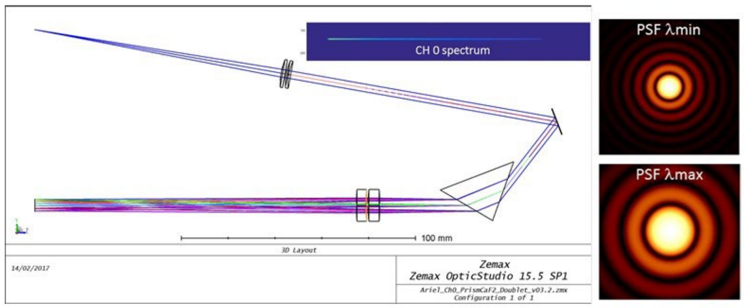

Figure 10. Zemax implementation of Channel 0 Spectrometer

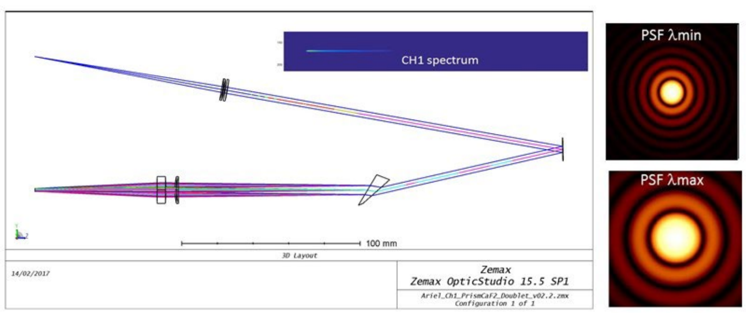

Figure 11. Zemax implementation of Channel 1 Spectrometer

6. AIRS COLD UNIT THERMAL AND MECHANICAL DESIGN

The mechanical design is based on two independent spectrometer half-boxes, each containing one channel, that are ultimately assembled together. The folding of the two channels in the volume is described in Figure 6. The full structure for the AIRS Optical Bench will be in Aluminium 6061 T651 to provide homothetic shrinking design at cold and good thermal coupling with the ARIEL PLM Thermal Optical Bench.

The overall maximum size of the volume is set by the CH1 longest arm. As the beam is collimated for both channels between the collimator and the camera, the design can easily be adapted for folding and matching length and alignment of both arms to a single plane for the entrance focal plane and for the detector focal plane. In the baseline case with 2 detectors, the folding of the system requires a single additional fold mirror on each channels path. The support holders for all the optical elements will ensure decoupling of CTE mismatch during thermal cool down and stiffness for vibration.
The AIRS-OB cools-down passively to 55-K through thermal conductance at interface with the ARIEL Telescope Optical Bench. This ensures minimal thermal noise on the Detection System. AIRS detectors are actively cooled to <42K by the Active Cooler System (ACS) based on a Neon Joule-Thomson cooler developed be the Rutherford Appleton Laboratory (RAL).

The dimensions of AIRS Cold Unit are displayed on Figure 12.

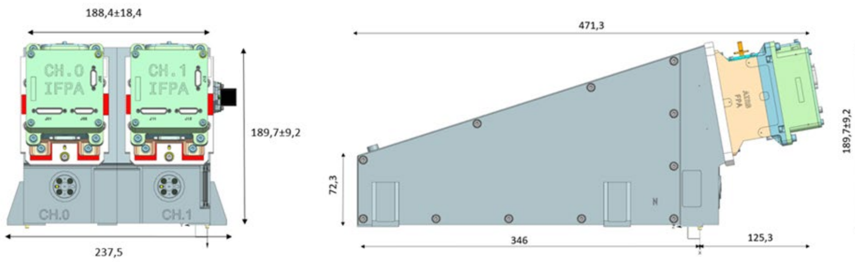

Figure 12. AIRS Cold Unit overall dimensions

The AIRS structure is fixed to the TOB by 7 x M6 screws. The positioning is obtained by 2 dowel pins. Each channel can be mounted and tested separately. The indexation of the two boxes is obtained by 2 dowel pins. Each channel is composed of one optical bench, one belt and one cover. Two adjusted holes are machined in each optical bench to make a mechanical reference parallel to the optical beam.

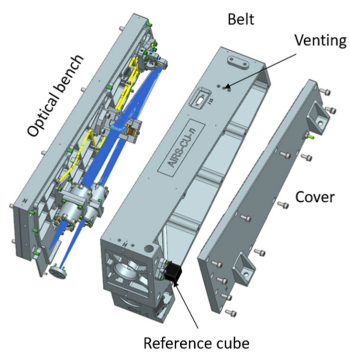

Figure 13. AIRS Cold Unit: Exploded view of CH1

6.1 Cold Tip Thermal Links routing

Current routing of the Cold Tip Thermal Links (CTLs) between both AIRS iFPAs and the ACS Cold Tip is presented in Figure 14.

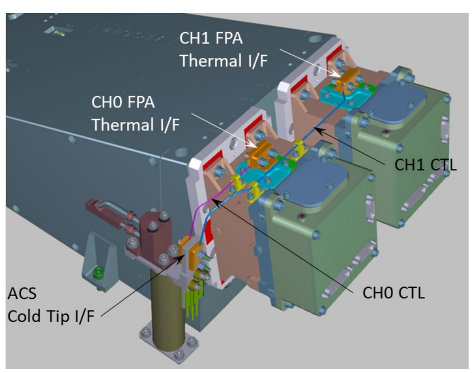

Figure 14. AIRS CTLs routing

Both FPAs are thermally linked to the ACS cold tip (at 32K) through 2 independents thermal links based on Aluminium wire. Each CTL wire cross section is defined as function of its length and the required temperature (below 42K) at detector level.

6.2 AIRS Cold Unit mechanical analysis

For mechanical analysis purpose at Cold Unit level, all optical elements (doublets, prisms assemblies, mirrors, detectors) and iFPAs, are modelled as lumped masses at their center of gravity. Their inertias are also filled in. They are attached to the OB with RBE3 elements. The CU Finite Element Model shown on Figure 15 is based on the current detail design considered as base line to manufacture the first prototype that will be used for mechanical and thermal qualification tests.

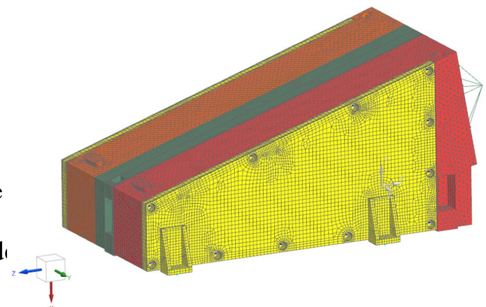

Figure

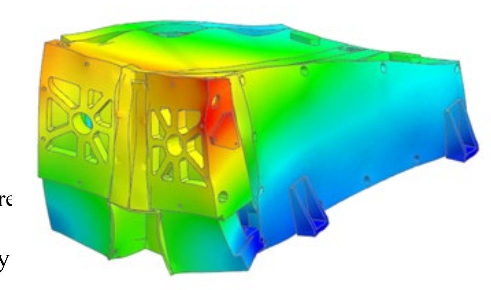

Figure

Figure 16 provid inly induced by that picture)

As summarized in Table 1, the analysis shows that first resonance frequencies with significant modal mass are above 140Hz at 850 Hz.
The behavior of the fasteners (M6 Inconel) at the interface of the TOB have been analyzed and all cases show positive margin. The fail-safe analysis also shows positive margins on sliding, gapping, yield and ultimate strength.

Mode n°	Freq (Hz)	Tx	Ty	Tz	Rx	Ry	Rz
1	859.21	0.07%	70.01%	0.01%	3.97%	0.00%	46.17%
2	1106.65	24.35%	0.05%	47.11%	11.14%	11.60%	10.73%
3	1160.30	0.43%	1.01%	0.00%	33.04%	0.32%	0.19%
4	1330.76	31.24%	0.05%	12.16%	5.66%	57.28%	12.41%
5	1392.14	1.90%	0.00%	3.60%	0.42%	0.28%	0.85%
6	1715.09	0.11%	4.12%	0.33%	1.60%	0.01%	0.86%
7	1780.36	0.05%	1.65%	0.06%	2.60%	0.09%	0.21%
8	1813.66	1.28%	0.04%	0.68%	0.67%	0.64%	0.67%
9	1842.09	0.04%	0.20%	0.46%	1.71%	0.19%	0.04%
10	1916.24	3.30%	0.03%	8.30%	2.94%	1.03%	1.35%
11	1951.53	3.79%	0.03%	8.00%	1.60%	0.03%	2.23%
12	1982.53	0.39%	5.88%	0.25%	1.36%	0.03%	0.17%
13	1998.70	4.95%	0.03%	2.92%	1.10%	0.57%	1.28%
14	2014.04	0.28%	0.55%	2.20%	0.70%	0.24%	0.01%

Table 1. Effective mass fraction for modes up to 2000Hz

Thermo-mechanical analyses were also performed to evaluate the impact of the temperature variation on the optical performances. Two cases were studied: a variation of +/- 1K around 55K to evaluate the stability of the OB and displacement of the optical dioptres between 45 and 60K.

The first one results in less than 0,1% variation in energy encircled in a 2 pixels radius, and the second to less than 1 % of the same criteria.

6.3 Doublet Design

There are 2 lenses per doublet. In the first doublet of channel 0, the first lens is in CaF2 and the second in Al2O3. Lenses are maintained in position by a spring pushing them against the mount. The aluminium 6061 mount is positioned on the AIRS optical bench by two pins.

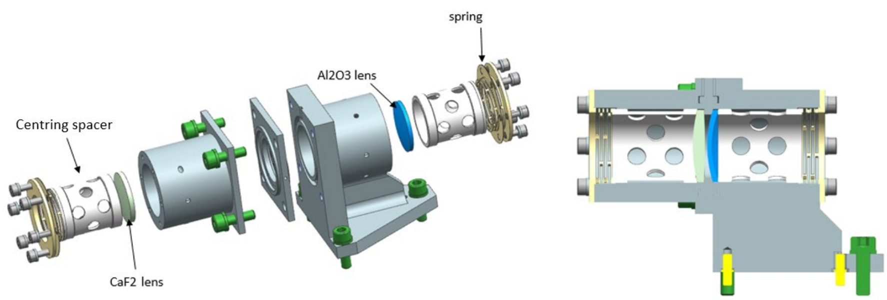

Figure 17. CH0 collimator doublet (CH0 D1)

The spring should apply a strength high enough to prevent the lens from losing contact with the mount during vibration tests. The mount is designed to maintain the lens at the center even with the thermal deformations. A chamfer is made on the mount for centring. A chamfer tangential to the lens is also made on the aluminium 6061 centring spacers.

The required load to be applied on both springs has been computed and thanks to finite element modelling the corresponding deformation and Von Mises constraints have been computed.

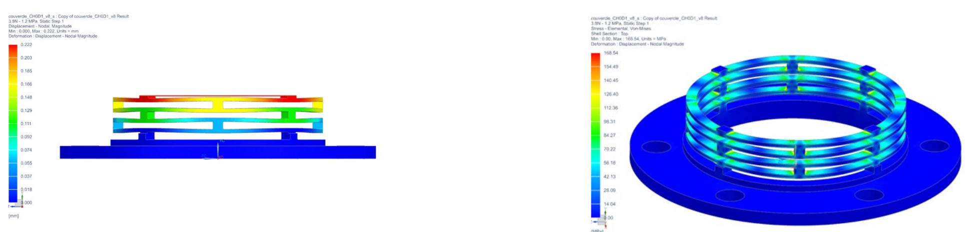

Figure 18. Displacement (left) & Von Mises Stress (right) of the spring under a 3.8N load

6.4 Prism Design

Both AIRS prisms are in CaF2 which is known to be brittle. Furthermore, CaF2 is birefringent, so it is important to avoid any stress in the use volume. However, CaF2 prisms and lenses have some return of experience in space programs at cryogenic temperatures (JWST-NIRSpec low resolution prism, with resolution similar to AIRS, JWST MIRIm filters). The dimensioning of the prism support and the design principle for channel 0 is described below, the same is applicable to channel 1.

To avoid birefringence, the two functions of the prism (optical and structural) are split in the design: the front part of the prism is the optical part and the back part is hold by the mount.

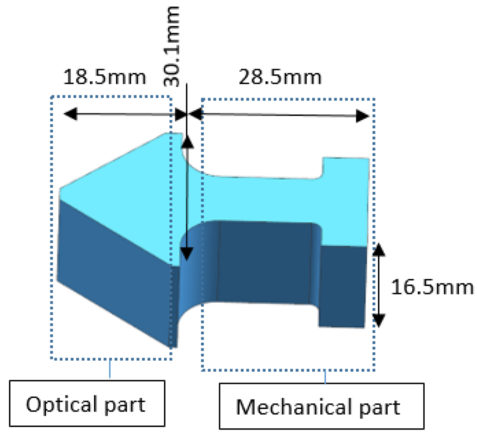

Figure 19. Prism channel 0 design

The prism is kept in position using springs and half-spheres (on Figure 20, springs are in orange, half-spheres in grey). Pads in Teflon are used at the interface between springs and prism (white on pictures). The heights of these pads will be adjusted to obtain the desired compression of the springs.
This system avoids to have too much stress in the prism:

- The 6 half-spheres provide an isostatic system;
- Pads have a large dilatation coefficient and avoid too much increase of the forces applied on the prism by the springs at 55K.

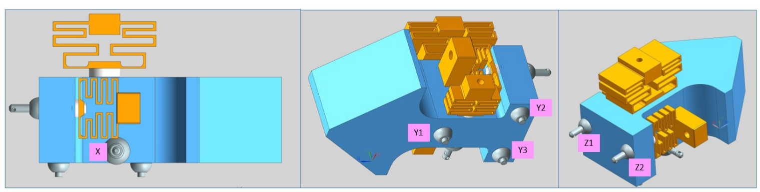

Figure 20. Prism with half-spheres and springs

To prevent differential dilatations with AIRS OB, the prism holder is in Aluminium 6061 T651. An angular adjustment is obtained with shims with a pitch of 0.013 degrees' accuracy.

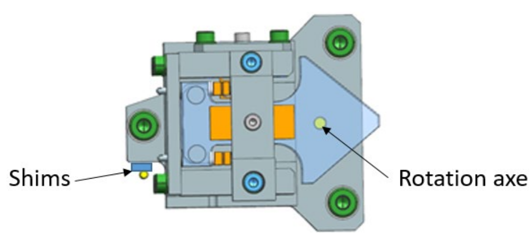

Figure 21. Prism in its mount (CAD)

6.5 AIRS integrated Focal Plane: iFPA

As for the rest of AIRS design, there are 2 independent iFPAs, one for each channel referenced I-FPA-CH0 and I-FPA-CH1. Those are mounted respectively on AIRS-OB CH0 and AIRS-OB CH1 and electrically linked to the CH0 and CH1 Detector Control Unit (DCU).

Each iFPA stands for integrated Focal Plane Assembly. It is the assembly that provides the following main functions:
- Thermal mechanical coupling to the AIRS-OB;
- Thermal mechanical support of the AIRS detectors;
- Support of the CFEE;
- Harness between the detector and the CFEE
- Thermal Control of the Detector;
- Thermal Control of the CFEE;
- I/F to the ARIEL Active Cooler Cold Tip
- Adjustment shimming of focus and relative spectrum / detector position.

The 2 AIRS iFPA are thermal mechanical boxes containing for each channel (CH0 and CH1):
- The Sensor Chip Assembly (SCA) with the detector and associated Read Out Integrated Circuit (ROIC), and the thermal control (2 temperature probes + 2 heaters per SCA). The SCA is mounted on a support plate thermally decoupled from the FPA mechanical structure and locally regulated through a thermal control at a temperature inferior to 42 K with a stability of +/-5 mK.
- The Cold Front-End Electronics (CFEE), linked to the Detector ROIC with a dedicated harness (Cryo Flex Cable CFC). The CFEE is regulated through a thermal control to +/- 50 mK.

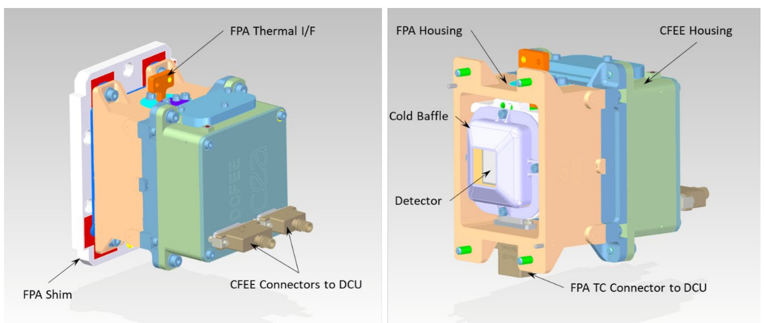

Figure 22. AIRS iFPA design overview

The iFPA box is made of aluminum 6061T6 in order to ensure good match and homotetic shrinking with the rest of the opto-mechanical system: the AIRS Optical Bench and the Telescope Optical Bench. Both AIRS iFPAs are equipped with a mechanical shim which is the interface between the iFPA and the AIRS-OB. Those shims allow adjusting the focus of the detector to the best focus of the optical system and adjusting the position of the spectrum on the best area of the detector.
The shim allows a displacement of +/- 9.2 mm of the FPA detector with respect to AIRS-OB optical interface sufficient to move the spectrum anywhere on the detector. The accuracy of location of the spectrum window with respect to the optical axis needs to be better than +/-5 pixels in order to locate accurately the spectrum into the selected window area (oversized by 10 pixels). This corresponds to an accuracy of +/- 90 µm. The axis of the columns, defined at SCA mounting level by fiducials, needs to be oriented with respect to the dispersion direction to better than 0.5°, which is largely feasible with a standard accurate pin interface.
The shims also allow for focus compensation which require the surface of detection to be located to +/- 50 µm in order to ensure optical performance. On a complex assembly like the FPA, with multiple mechanical stages, this can only be done by accurate shimming of the I/F plate following metrology of the location of the SCA with respect to the FPA mechanical interface.

The cut view of the iFPA provided in Figure 23 allows to identify all the key elements that constitute the iFPA. One iFPA is the assembly of 2 sub-assemblies: the FPA that includes the H1RG detector (provided by TIS) and the CFEE that implements a differential pre-amplification stage and filtering functions (See section 7). Both sub-assemblies are mechanically assembled and electrically connected thanks to a custom made cryogenic flex ribbon cable.

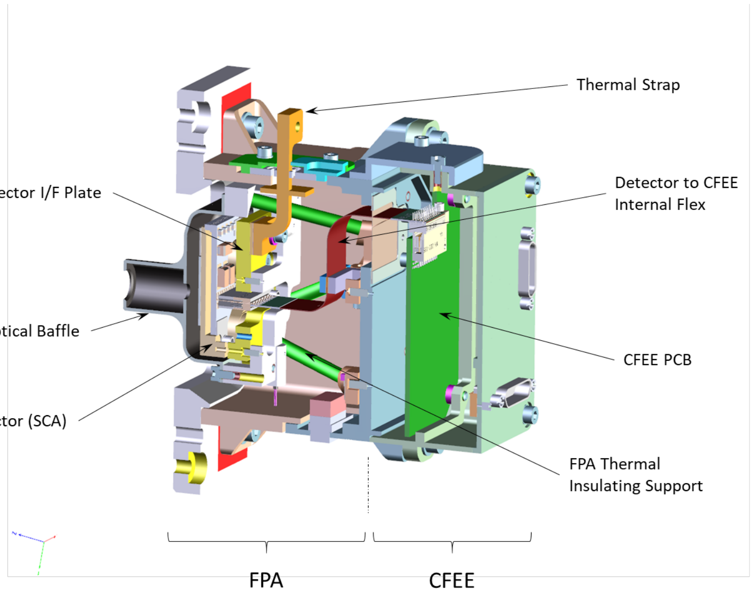

Figure 23. Cut view of the iFPA

The support structure holding the SCA Block inside the FPA housing is based on a GFRP hexapod in order to allow good structural behavior in vibration and accurate positioning while ensuring correct thermal decoupling of the 42K stage from the 55K main bench. The selected material is leading to a total thermal parasitic load from the FPA structure toward the SCA below an allocation of 10mW.

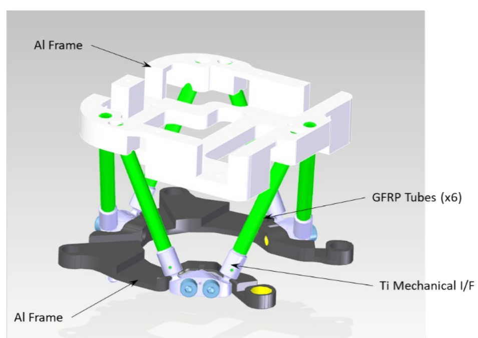

Figure 24. FPA Hexapod Thermal Insulating Support

As depicted in Figure 24, the FPA Thermal Insulating Support is based on 6 GFRP tubes of 4 mm outer diameter and 2.5 mm inner diameter. At one end, those tubes are bonded inside a Titanium frame, while at the other end they are directly bonded in an Aluminium frame. The free length for each tube is 30 mm, that allows to control and keep the thermal parasitic load flowing to the Detector below the required level. The Titanium frame design allows to adjust the first eigenfrequency of that insulating support in the required frequency range in order to avoid mechanical coupling with the Cold Unit Optical Bench.

All along the design phase, a finite element model (FEM) of the full iFPA has been used to performed mechanical analysis and validate the design with respect to overall requirements and limitations from sensitive elements.

One of the main design driver is the maximum acceleration at Detector level. This is mainly driven by the design of the thermal insulating support. Therefore, the mechanical analysis results presented here after focus on that element while the CFEE is only considered as a lumped mass. This mechanical design is the result of an optimization balancing both, mechanical and thermal performances.

We present here after some of the main results issued from the modal and random analysis. The Table 2 summarizes the results of the iFPA modal analysis.

	f (Hz)	Effective mass (%)
FX - mode 2	165	38
FY - mode 1	158	38
FZ - mode 3	423	41

Table 2. Summary of the iFPA main modes

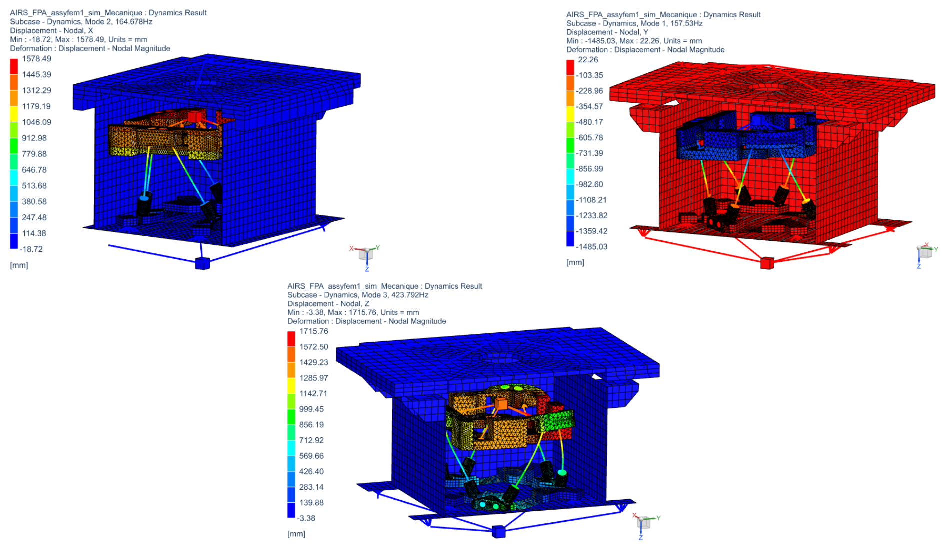

Figure 25. FPA main Mode, top left: in X direction Mode 2 : F=165Hz, top right: in Y direction Mode 1 : F=158 Hz, bottom: in Z direction Mode 3 : F=423 Hz

Random analysis have been also performed. As an example, the Figure 26 provides an overview of the spectral response in X axis at both levels: Detector and Cold Front-End electronics, superimposed on the input spectrum derived from the specification at Telescope Optical Bench level.

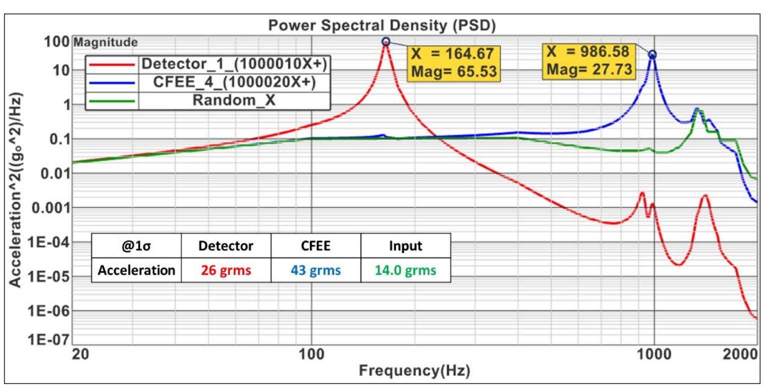

Figure 26. Detector and CFEE spectral responses in X axis

In parallel thermal analysis have been performed in order to demonstrate that all thermal requirements was met over the full temperature operating range defined for AIRS. We present in Figure 28 the simplified thermal model of the iFPA with all representative thermal links. This model have been intensively used both to make a sensitivity study with respect to the different thermal links and to check, through transient analysis, the capacity of the thermal control loops to obtain the required temperature stabilities at the detector and at CFEE levels.

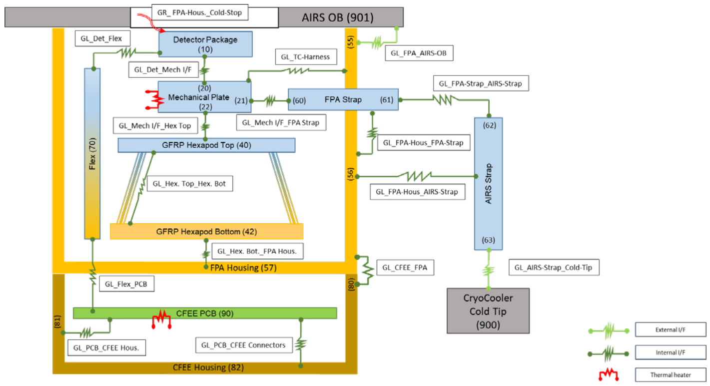

Figure 27. iFPA Thermal Model Synoptic

7. AIRS DETECTION CHAIN ELECTRONICS

7.1 Electrical System Overview

The electrical system of the AIRS instrument is composed of:

- The two FPAs (CH0 and CH1) including electrical parts for temperature stabilization of the detectors;
- The two CFEE units; one for each detector channel (CH0 and CH1) including electrical parts for temperature stabilization of CFEE;
- The two Detector Control Unit (DCU) sub-assemblies; one for each detector channel (CH0 and CH1), assembled as the AIRS DCU (A-DCU).

AIRS electrical architecture is the assembly of two independent and complete channels, started from the detector and ending with the AIRS-DCU. Only FPA channels differ, in term of spectral range while cold electronics (also named CFEE) and DCU for both channels are identical. No redundancy is implemented in the channels to the exception of focal planes thermal control that are duplicated. The A-DCU is then interfacing to the Command and Data Processing Unit (CDPU) of the Instrument Control Unite (ICU) for scientific & housekeeping data transmission and for the transmission of configuration command. It interfaces with the Power Supply Unit (PSU) that is providing secondary voltage lines including a low noise line for detector and CFEE feeding which is mandatory for adequate control of performance at detector level. These interfaces with the ICU sub-assemblies implements cross-strapping to enable coupling of both AIRS channels to redundant functions of this unit.

Figure 28 is a representation of this electrical system.

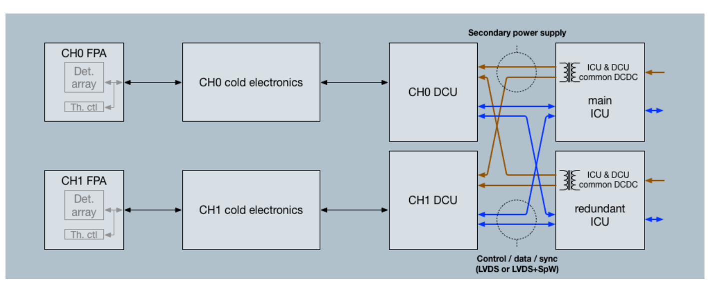

Figure 28. Overview of AIRS Electrical System

The full electronics chain is submitted to various environmental conditions. Detectors are operated at low temperature condition (<42 K).
The CFEE based on discrete components is compatible with a 55 K operating temperature and located very close to the detector (<100 mm). DCU is operated at ambient temperature condition (Operating temperature between 253 K and 313 K and stability +/-3 K over 10 hours) on the SVM. Additionally, cryoharness make the links respectively between the cold sub-systems and between the CFEE and the A-DCU.

Preamplification for the ROIC output 'video' signal is implemented into the CFEE. Others functions such as the readout clock sequencer and bias generators are moved into the warm electronics A-DCU.

Figure 29 illustrates the distribution of functions between the A-DCU and the CFEE in the baseline.

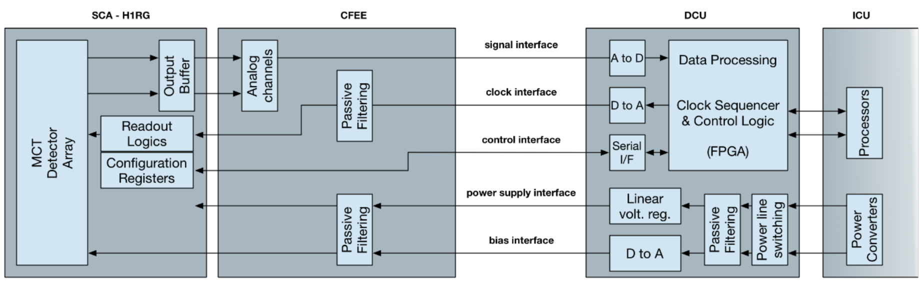

Figure 29. Discrete Components Electronics Option

Figure 30 depicts the electrical block diagram of the instrument, including all the sub-systems and the different harness stages.

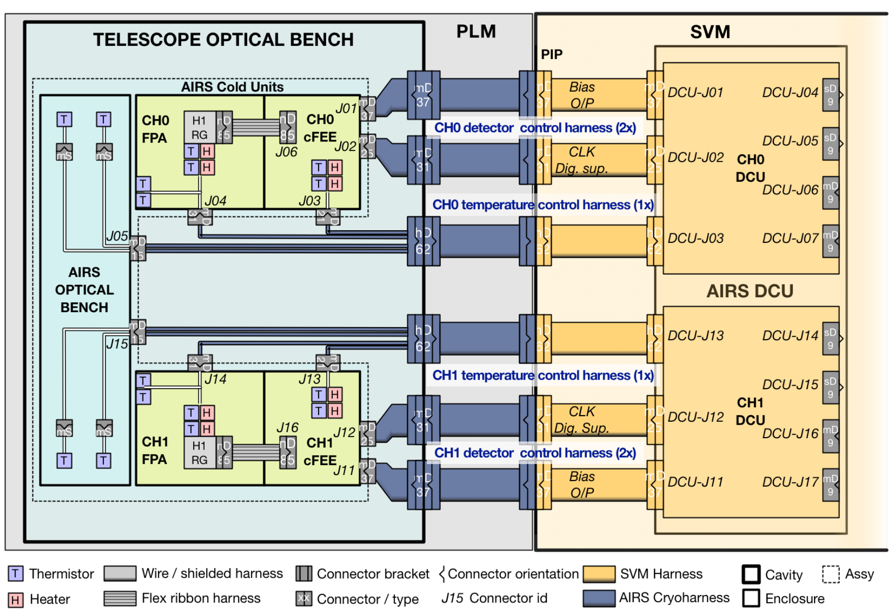

Figure 30. AIRS Electrical Block Diagram

Electrical design of the A-DCU encompasses several high-level functional blocks either analogue or digital. Figure 31 is a representation of the block diagram of the unit along with corresponding functions of the CFEE.

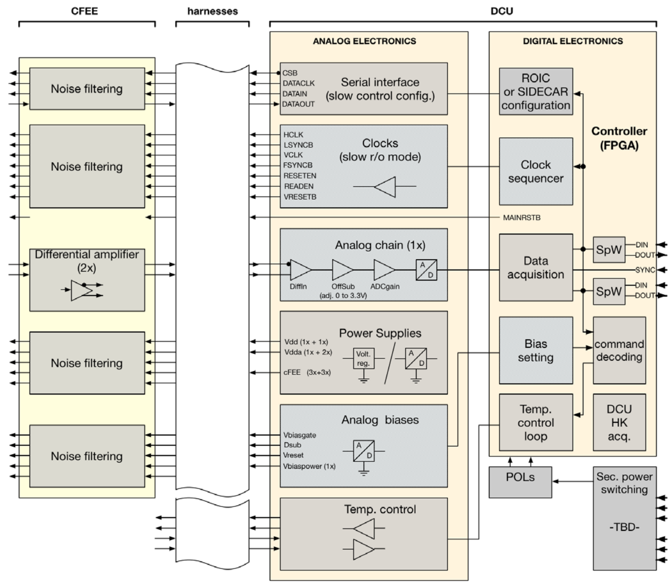

Figure 31. A-DCU Electrical Block Diagram

AIRS Electrical Architecture defines 6 electrical interface signal families:

- Bidirectional digital interface (3-wire type);
- Detector clock output signal interface;
- Analog signal input interface;
- Power supply output interface;
- Bias voltage output interface;
- Thermal control.

7.2 AIRS DCU design description

An overview of the analogue control electronics for the detector readout is represented in Figure 32. On the top of the figure the analogue chain is represented from the CFEE unit (on the left) to the A-DCU unit (on the right). The remaining functions represented in the scheme correspond to the signals for driving the detector. It is encompassing fixed bias voltages, adjustable bias voltages and clock signals for the execution of the detector readout sequence. Fixed bias signals are very low current supply lines for the detector assembly (detector + readout circuit). Adjustable bias signals are necessary to bias the diode-based detector and few operating condition of the readout circuit. Finally clock signal are provided to the readout circuit to implement the Teledyne H1RG slow readout mode.

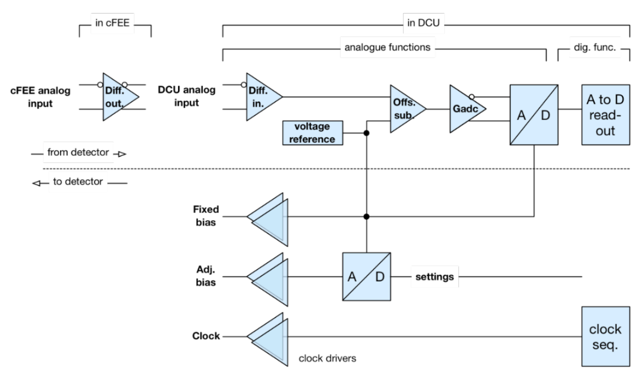

Figure 32. Analogue Control Electronics – Discrete Electronics

Analogue signal processing chain is split into three sub-assemblies with ROIC output signal on the left and digitization on the right of the Figure 32. In the middle of the chain the signal is pre-amplified by the CFEE that allows signals to be transmitted along meters-long harnesses.
A full analogue chain modelling using SPICE tool has been performed in order to validate the preliminary design. The model includes the preamplifier for the CFEE, the differential amplifier, an offset suppression amplifier, an ADC driver and a simple model of the sampling stage of the ADC. Preliminary result of noise simulation gives estimated in the white noise region around 10 nV/√Hz and 1/f knee is between 2 to 3 kHz.

An FPGA is implementing all the digital functions of the A-DCU. It encompasses:

- Reception of low-level commands from ICU for configuration and operation;
- Transmission of packet of data either of scientific type or housekeeping type (inc. cryogenic temperature monitoring channels);
- Control of the analogue electronics functions:
    - Science ADC and scientific ADC;
    - Detector bias voltage setting digital to analogue converters;
    - Temperature regulation heater bias current setting digital to analogue converters;
- Generation of detector readout clock cycles;
- Execution of a temperature regulation loops; one for FPA and one for CFEE – Target temperature is set by mean of a low-level command. Status of the control loop is reported as housekeeping parameter.

Exchange between the A-DCU and the ICU is relying on a SpaceWire link and the implementation of the RMAP protocol.
Considering previous designs, it is foreseen to select a Microsemi FPGA from the RTAX family (RTAX2000) as a target for the implementation of all the DCU logical functions.

The A-DCU is based on following mechanical implementation:

- Printed Circuit Boards are parallel to the SVM Panel I/F;
- 2 independent frames stacked on a Base Plate used as thermo-mechanical I/F + a Cover;
- Connectors are located on two opposite sides. One side is dedicated to harnesses connected to the AIRS CU, opposite side is dedicated to the ICU connections (Power supply and SpW).

Figure 33 gives a 3D view of the A-DCU box

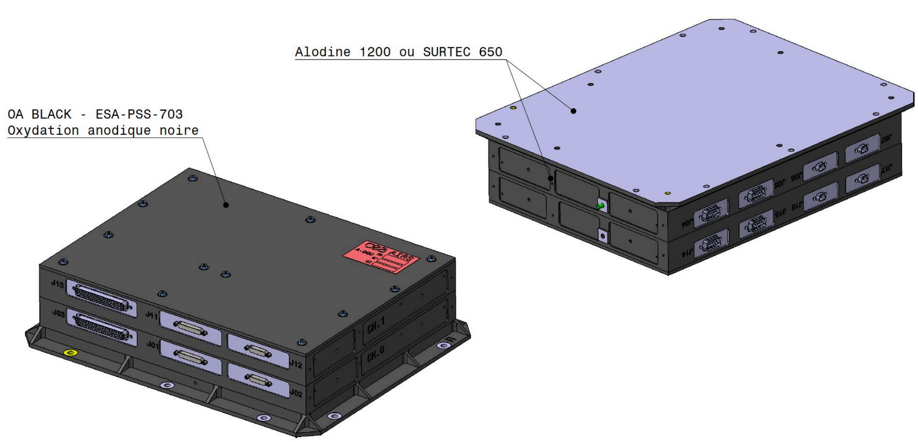

Figure 33. A-DCU Box mechanical layout (overall dimensions: 327*257*85 mm^3, mass (CBE) = 4.4kg)

8. PROTOTYPES AND TESTS

8.1 Optical sub-assemblies

Bread board model of all optical sub-assemblies will be manufactured and tested before the development of the EM.
The first sub-assemblies to be tested were the prism for CH0 and CH1 as they were considered the riskiest designs. Both prisms and in their mount have been successfully tested in vibration and underwent 8 thermal cycles between 37K and 323K.

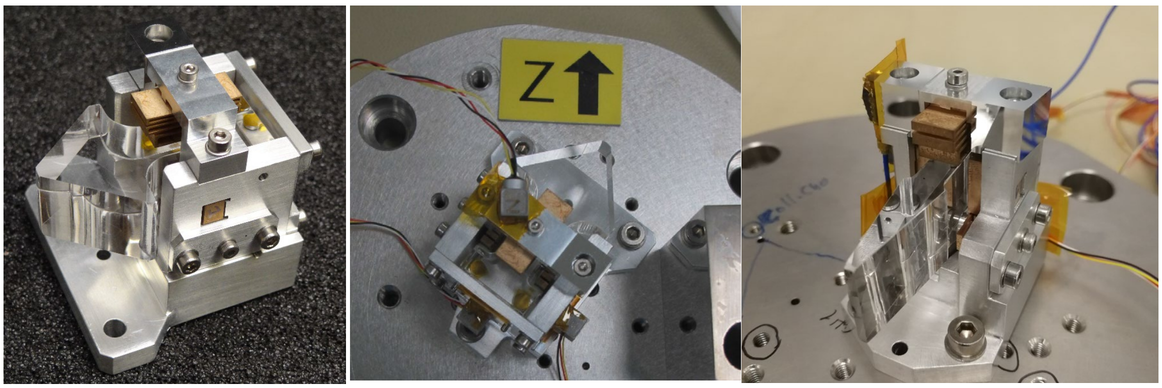

Figure 34. left: First prototype of CH0 prism assembly – center: CH0 prism assembly in vibration test configuration for design validation – right: CH1 prism assembly during vibration test

For CH0 prism, the first mode happens around 1550Hz which is in good accord with the FEM prediction. It has been also demonstrated that the motion of the prism was well controlled and its nominal position kept in the tolerances after the vibration runs.
The thermal cycling test led to a minor modification of the mount to minimize the CTE difference and keep the prism in its nominal position.
Both designs are now considered consolidated
For the doublets sub-assemblies, the collimator of CH0 (CH0 D1) and the camera of CH1 have been manufactured and assembled.
CH0 D1 has been successfully tested in vibration and thermal cycling. The concept of the mechanical design of all doublets is identical but as the sizes, dimensions and material of the lenses are different, all doublets shall be tested.

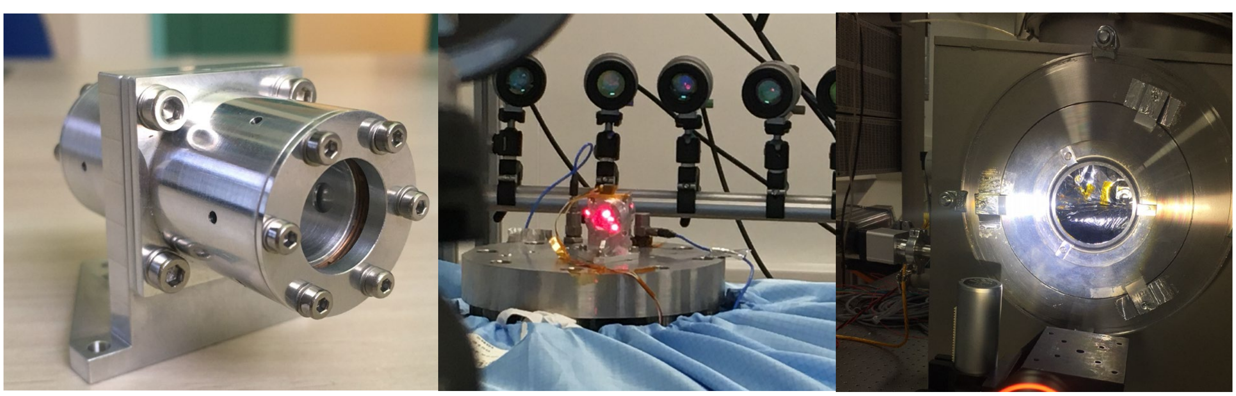

Figure 35. CH0 D1 bread board model - left: assembled - center: during vibration test - right: during thermal cycling

In the near perspective of the mechanical test of the AIRS Cold Unit Structural Model, all main structural parts and mass dummies have been manufactured. It is important to note that all those parts are considered very close to the final design and only very minor modifications are expected.

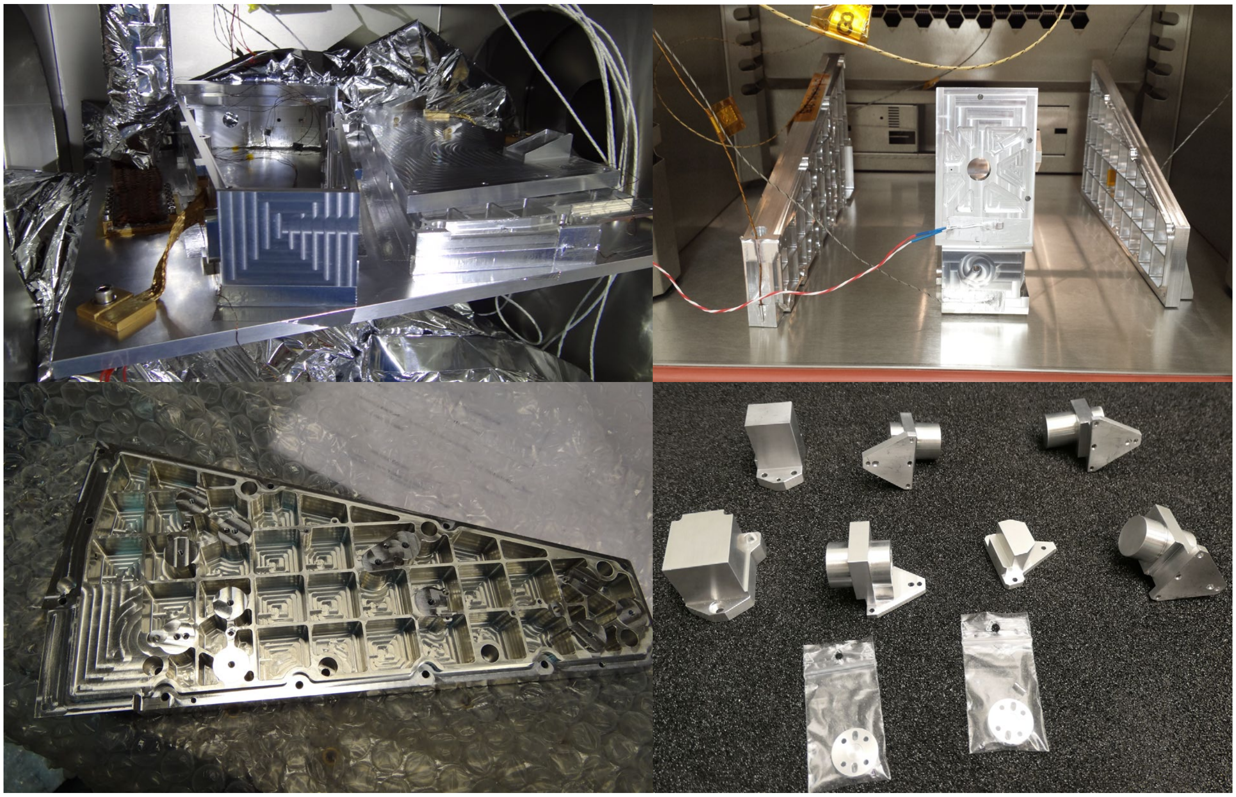

Figure 36. top left : STM structure part during stress relief cold cycle - top right : during hot cycle - bottom left : CH1 Optical bench after final machining - bottom right: optical sub-assemblies mass dummies for STM.

8.2 integrated Focal Plane Assembly: iFPA

In order to validate the mechanical design of the detector insulating support (hexapod) identified as one of the critical item of the FPA assembly, a bread boarding program has been initiated very early in the project. Some months ago, few of the so called hexapods have been assembled and vibration tests have been successfully performed (see Figure 34). Following this first design validation step, few sets of iFPA mechanical parts have been manufactured and one full iFPA structural model have also experienced a vibration test (Figure 34). Some additional tests will undergo in the next months in order to optimize the mechanical behavior and reducing amplification factor at detector level. However those preliminary tests are very encouraging and the expected modifications still minors.

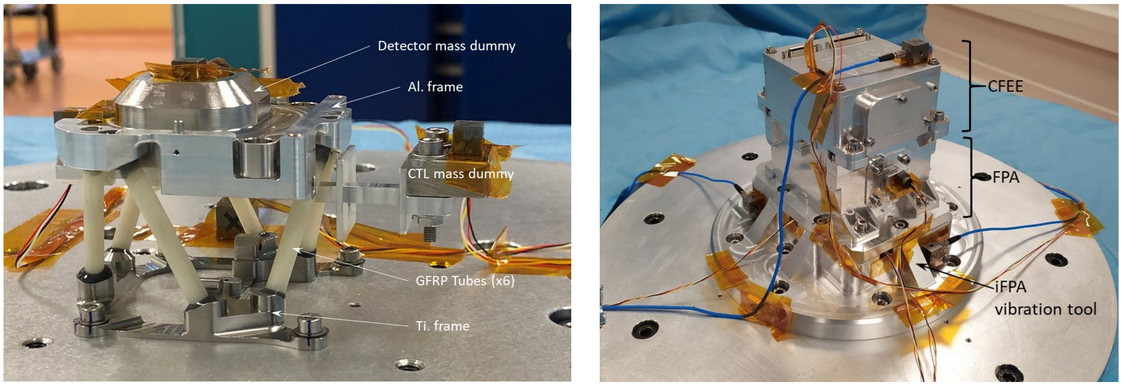

Figure 37. left: First prototype of the detector insulating support assembled on the shaker - right: Full iFPA structural model assembled on the shaker

8.3 A-DCU prototype

A prototype of the A-DCU has been developed and fully tested. It is now ready to be used as an EGSE (Electrical Ground Support Equipment) and connected to the H1RG detector. This will represent an important milestone for the AIRS detection chain development program, as it will allow to validate the full detection chain in flight configuration.

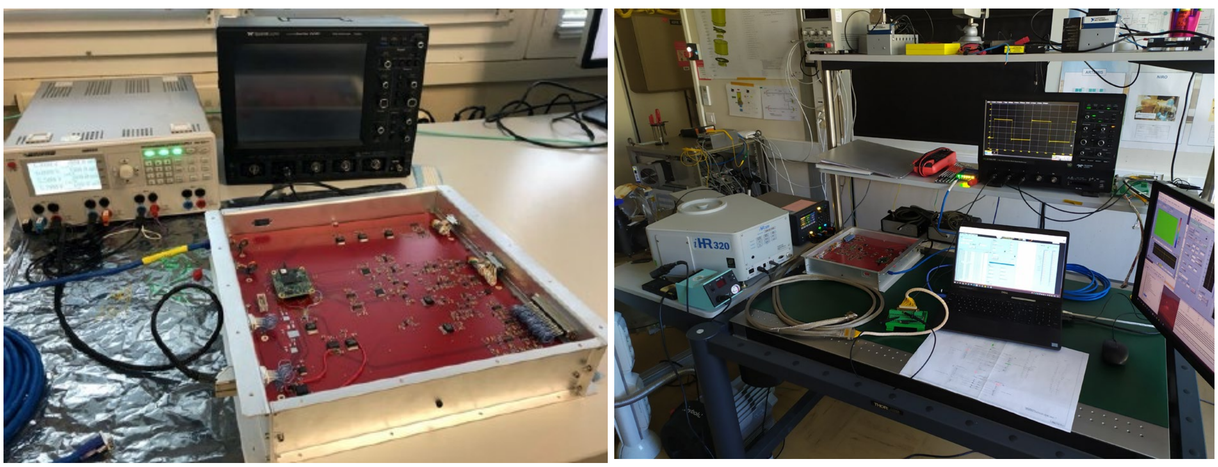

Figure 38. Left: A-DCU Bread Board Model during test phase – Right: View of the A-DCU used as an EGSE connected to the detector calibration test facility (located in the left, not visible on the picture)

8.4 CH1 Detector Tests

A detailed description of the AIRS detectors is published in another paper of this proceeding [10]. For the sake of consistency, a brief description is presented below.

AIRS detectors are 1024x1024 pixels HgCdTe-based detectors manufactured by Teledyne Imaging Sensors. These detectors are widely used in astrophysics in the IR domain. The light sensitive layer, made with HgCdTe material, is grown on a CdZnTe substrate. The HgCdTe bandgap (hence the targeted cutoff wavelength) is tuned by varying the amount of cadmium in the alloy. The detection layer is hybridized onto a silicon ReadOut Integrated Circuit (ROIC) via indium bumps. The ROIC is based on Source Follower per Detector (SFD) architecture. The detector is reset at the beginning of an integration. As the signal is accumulating in the diode space charge region, the diode capacitance discharges, and the voltage applied on the gate of the pixel source follower is changing, modifying the measured output signal. With this ROIC architecture it is possible to operate the detector in different readout mode either CDS (Correlated

Double Sampling) or FUR (Following up the ramp). Depending on the brightness of the target observed one of these readout modes will be chosen. In any case, the detector will be operated in photon noise limited regime. Key detectors requirements are reported in Table 3.

	CH0	**CH1**
Targeted window size	355x64	130x64
Spectral domain	1.95 µm – 3.90 µm	3.90 µm – 7.8 µm
Median dark current	0.01 e-/s/pix	1 e-/s/pix
Median CDS readout noise	22 e-	23 e-
Full well	> 100 000 e-	> 50 000 e-
Mean QE over spectral domain	> 60%	> 60%

Table 3. AIRS detector requirements for each channel

Both AIRS detectors are operated in buffered mode, in one output, and in window mode. These operating modes are selected by programming dedicated internal registers of the detector. The pixel rate is equal to 100 kHz. For CH0, the window size is equal to 355x64 pixels whereas for CH1 the window size is set to 130x64 pixels. During detector operation, the pixels out of the window of interest are not read. Although they should not see any photons, they will have to be regularly reset during observations, to prevent them from becoming saturated and then disturb the pixel in the science window.

Moreover, the acquisition chain makes use of the separate reference output of the H1RG detector which is a completely independent output channel of the detector. This reference output is associated with a reference pixel with a capacitance value of 40 fF. This separate reference pixel is different from commonly used reference pixels located on the edges of the detector array. In our case, this output is kept at Vreset during detector operation.

At CEA, we have developed a test bench dedicated to the characterization of the detector of both channels. This test mean allows the characterization of the detector in dark and under illumination at their operating point (around 42K). First characterization results were acquired within this test bench, on an early engineering model of CH1 detector lent by ESA. Details of the characterization results are published in paper number 12191-81 of this conference's proceedings. A map of the dark current and the associated histogram are shown on Figure 39. The median dark current is equal to 0.070 e-/s/pix which is well below the median dark current requirement equal to 1 e-/s/pix.

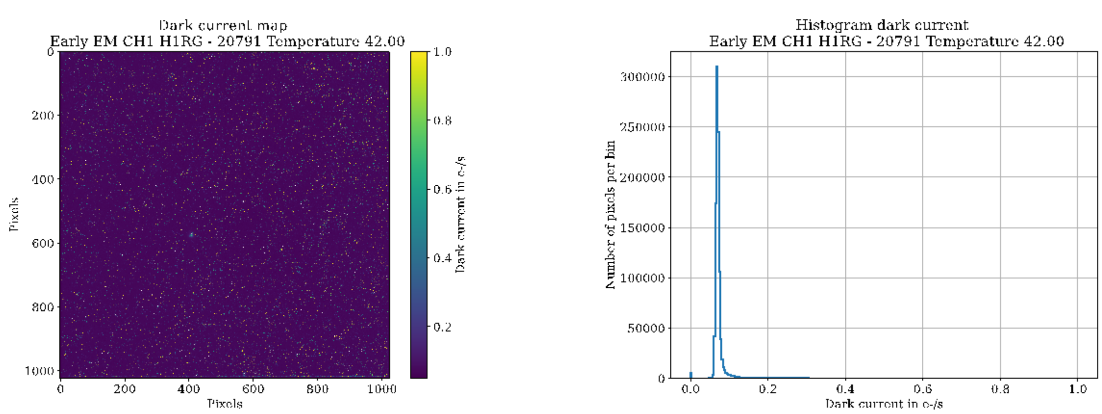

(a) (b)

Figure 39. Dark current map (a) and dark current histogram (b) measured on H1RG detector at 42 K

8.5 AIRS calibration test facility

The AIRS instrument will be tested into the SimEnOm facility at LESIA (Paris Observatory). The setup, as depicted in Figure 40, is designed with 5 regulated thermal sinks inside the vacuum chamber. The main SimEnOm optical bench is cooled down to 173 K with a nitrogen circulation. A first thermal shroud mounted on this interface is cooled down to 80K also with a nitrogen circulation, and a second one is cooled down and regulated from 42 to 60K, thanks to a thermal link to a 25 K cryocooler.

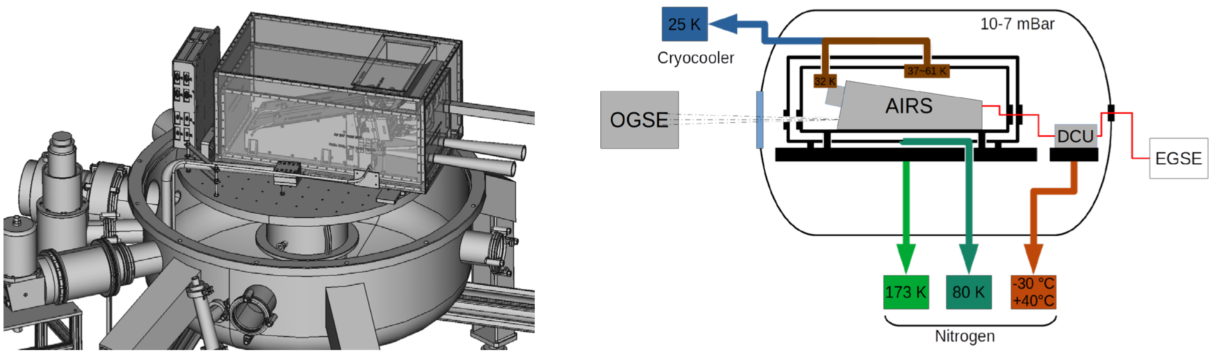

Figure 40. Right: CAD view of AIRS instrument inside the 2 thermal shrouds on the main SimEnOm optical bench. Left: AIRS test configuration scheme: 2 thermal links toward the cryocooler (top right), OGSE and optical feedthrough (right), EGSE electrical feedthrough (left) and 3 independent thermal sinks cooled by nitrogen circulation (bottom).

AIRS cold unit is mounted inside the coldest thermal shroud that reproduces the thermal environment in PLM flight configuration. A cooper mass also linked to the 25 K cryocooler, ensures a regulated temperature of 32 +/- 15 mK to reproduce ACS cold tip interface linked to the detectors.

The A-DCU is connected to an independent thermal sink, regulated to warmer temperature from -30 to 40°C.

The SimEnOm vacuum chamber is equipped with a CaF2 window, so the OGSE is outside on the dedicated optical bench. CH0 and CH1 slits can be seen through the window as well as the alignment cube for alignment purpose.

As depicted in Figure 41, the OGSE optics is designed to offer a focused beam with an aperture of f/12 (f/18 in the spectral direction). The off-axis parabola are illuminated with a monochomator (TMS300), or a black body (HGH RCN1350N1 (50°C-1350°C)) through a pinhole. Mounted on a hexapod, the input beam has degrees of freedom in translation, tip-tilt, and focus to cover the range of alignment to test.

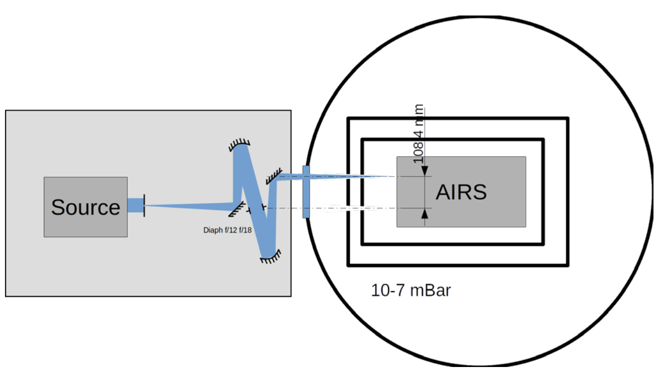

Figure 41. OGSE configuration

The OGSE will only illuminate one channel at time. A cold stop is put in front of the second input to measure the background. A neutral density filter will be put in front of the illuminated entrance, to reduce the thermal background to a level comparable to the dark level requirement (10^{-4} for CH0, and 10^{-6} for CH1).

9. CONCLUSIONS AND FURTHER WORK

The AIRS instrument design is now stable and thanks to the early development and characterization of critical subsystems through bread boarding programs, most programmatic and technical risks have been minimized. All this work has been made in the perspective of the iPDR to be held at the end of this year, 2022. The AIRS Cold Unit structural and thermal model planned to be assembled and tested in Q4 2022 will be an important milestone in the design validation for the instrument CDR scheduled early in 2024. In parallel to the validation program of the cold unit, a dedicated program of development for the A-DCU will be conducted in order to validate all aspects as electrical, mechanical and thermal. Dedicated A-DCU models are planned to be manufactured as function of the tests to be performed. The A-DCU program will also be key for the validation of the performances of the full AIRS detection chain split between A-DCU and iFPA connected with flight representative cryoharness.

10. ACKNOWLEDGMENTS

AIRS is the result of the collaboration between many French and European institutes. We wish to thank here all the collaborators from the IAS, LESIA, IAP, CEA and CNES, our common funding agency. This work would also not have been possible without the constructive interactions with the PLM project team at RAL who leads the AMC, the ESA team in charge of the ARIEL mission and the Airbus team prime contractor of the ARIEL spacecraft.

REFERENCES

[1] Forget, F., Leconte, J., Phil. Trans. Royal Society 372, #20130084, 2014
[2] Borucki, W.J., et al., Science, 325, 709, 2009
[3] Majeau, C., Agol, E. and Cowan, N. B., ApJ 747, id L20, 2012.
[4] Pace, E. et al, “ The telescope assembly of the ARIEL space mission”, these proceedings, 12180-36, 2022
[5] Konrad, R. Skup et al., “ARIEL fine guidance system: design, challenges, and opportunities”, these proceedings, 12180-38, 2022
[6] Morgante, G., et al., “The thermal architecture of the ESA ARIEL payload approaching the end of the phase B2”, these proceedings, 12180-192, 2022
[7] Noce, V., Focardi, M., et al, “The instrument control unit of the ARIEL payload: design evolution following the unit and payload subsystems SRR (system requirements review)”, these proceedings, 12180-196, 2022
[8] Di Giorgio, A.M., et al, “Instrument control data processing Software for ARIEL ICU”, these proceedings, 12180-197, 2022
[9] Hills, M., Crook, M., et al., International Cryocooler Conference, Inc., Boulder, CO, 2021
[10] Pichon, T., et al., “ARIEL early engineering model H1RG IR detectors: first characterization results”, these proceedings, 12191-81, 2022